A Review of the Use of Electron Beam Machines for Thermal Milling

G. BROWN,* K. G. NICHOLS
Department of Electronics, Southampton University, Southampton, UK

The factors which influence the size of the heat-affected zone of a material on which a focused electron beam is incident are reviewed. These include the limitation of current density in the focused spot, which is given by the Langmuir relation, and also the limitation imposed by the spherical aberrations of the lens which focuses the beam. The peak temperature rise in the material, with due allowance for the source penetration and backscatter effects, is discussed. The design requirements for electron beam machines are then considered. These are followed by brief descriptions of a number of machines which have been used for the machining of thin films, deposited on substrates, and for the machining of self-supporting thin foils. The principal features of the machined films and foils are described. The review concludes with an account of the various explanations which have been put forward to account for the observed experimental results.

Editorial Introduction

One of the most rapidly advancing materials processing techniques (at the present time) involves the use of "electron beam machines". The applications of these machines fall into a number of distinct categories, including machining (cutting and milling) operations and welding applications, use of evaporation sources, etc. The implications of the development of these techniques in materials technology are considerable – particularly in view of the ease and speed with which the beam can be deflected electrically to different parts of the work surface.

The precise design of the machine will differ from one application to another and to a large extent a discussion of the design of the machine is inseparably related to the processes which the beam is required to induce in the work material. The machine design and the materials problems must thus be considered together, and it is apparent that to date the former aspect of the problem has received more attention than the latter.

Many papers on the subject of electron beam machines and their applications have been published and a review of the entire field would

not only be of undue length but would, in many respects, be inappropriate, for the actual materials processes occurring in the various classes of application differ widely. This paper is the first of a number of papers which will be published in this journal from time to time reviewing selected aspects of this field. Its subject "The Use of Electron Beam Machines for Thermal Milling" is of great potential importance in the processing of thin films, particularly in microelectronics technology, and illustrates one class of application where thermal processes in the material are dominant. The object of the review, as well as to describe the present state of the art, is to guide the reader to the more important sources of information available and the references quoted have been chosen with this in mind rather than with the object of being completely comprehensive.

It will be apparent that this is a field in which many of the phenomena which occur are likely to provide interesting material for research for some years to come.

1. Introduction

The growth of electron beam technology during

*Now of R A E, Farnborough, Hampshire, UK

the last decade has been such that it is no longer possible to review all aspects of the subject within one short article. Quite apart from questions of length, it is not convenient to consider all applications of electron beam technology in the same review. This is because the nature of the application influences the basic design principles of any electron beam apparatus. The subject may be divided into a number of categories which, however, overlap to some extent. These are the use of beams for, *milling* or *cutting*, *welding*, *heating materials for vacuum deposition*, *vacuum purifications of materials*, and for *inspecting, examining and analysing* materials. In the last category, electron microscopy and X-ray microanalysis would be included. The first category is conveniently subdivided into *thermal* methods of milling or machining and into electron-beam-assisted chemical methods. These latter processes are commonly referred to as *non-thermal* methods of machining. The present review is restricted to thermal milling; non-thermal methods and the other categories of electron beam applications are not considered.

The use of electron beams for thermal milling and welding, stems from the pioneer work of Steigerwald and his co-workers [1] which culminated in the production of the first commercial machines.* These machines use the Steigerwald [2] long focus electron gun and have a long working distance from the final lens. In most subsequent machines simple triode guns are used and they have shorter working distances.

The basic arrangement of every type of machine is the same. Electrons from a tungsten hairpin cathode are focused into a *cross-over* spot by the electron gun. An image of the cross-over spot is then formed by a magnetic *objective lens*, or lenses, on the work material. The machines are designed such that there is sufficient power density in the final image to melt and possibly vaporise the work material. Conduction of heat away from the irradiated spot is the principal cause of loss of efficiency in the heating process. As will be considered subsequently, at a given beam power it is advantageous to work with as small an image as possible in order to minimise conduction loss. However, this is not always convenient, for reducing the spot size will also reduce the rate of machining. The actual process of machining is considered in a later section. It is

shown in the next section that peak temperature attained by the work-piece is, very approximately, proportional to the beam power and inversely proportional to the image diameter. Thus, an increased spot size implies that an increased beam power is necessary. However, it is worth noting that this means that the peak temperature increases in proportion to the spot diameter, provided the power density in the beam is constant. It is this which shows that coarse machining with a rapid rate of material removal is possible.

The effective heat conduction loss can also be reduced by the expedient of pulsing the beam. The principle here is that the material at the focused spot can be heated to high temperatures before any appreciable conduction of heat can take place. This follows because the rate of absorption of energy of the material at the spot is limited only by the beam power, while the rate at which the temperature disturbances can be propagated out from the spot is limited by the thermal diffusivity of the material; the high conduction loss does not occur until this disturbance has been propagated out some way. Pulsed beam operation thus leads to an increase in the efficiency of the heating process, the mean rise in temperature of the work-piece as a whole being less than that for the case of continuous beam operation at the same power. In addition, the sharper temperature profile associated with pulsed beam operation might be expected to reduce spot fringe effects in the machining process, with consequent increase in precision, although it is possible that thermal stress effects in the work material may be more serious in certain cases.

2. General Design Considerations

The design of an electron beam milling or welding machine is dependent on many factors. Of first significance are the dimensions of the heat-affected zone produced by the beam impinging on the work material. It is first necessary to define this zone. Wells [3] defines the dimensions of this zone by the rms diameters of the resultant temperature distribution on the surface and along the axis of the beam in a direction normal to the surface. For the latter diameter, it is necessary to postulate a hypothetical temperature distribution above the surface of the work material

*In reference 29, Steigerwald explains that his work on electron beam machines commenced in 1948 and he shows two photographs of prototype machines in operation in 1950 and 1952. However, the first paper on the topic was that due to Steigerwald in 1960, reference 1.

which is the mirror image of that below the surface. The usefulness of this definition depends on the form of the temperature distribution. Thus, if this form is known, knowledge of the rms diameters enables the zone of the material with temperatures above a certain fraction of the peak temperature at the centre of the distribution to be defined. The dimensions of the heat-affected zone, and its temperature distribution, depend, in a complex way, on the energy of the incident electrons, the current in the beam, the diameter and distribution of the beam in the focused spot, and the nature of the target material being worked. Referring to the latter factor, the thermal diffusivity and thermal conductivity determine the rate of growth, under transient conditions, and the final dimensions, in the steady state, respectively, of the heat-affected zone. In addition, the effective atomic number of the material and the energy of the incident electrons determine the degree of penetration of the beam into the material and the fraction of the incident energy lost by back-scattering of the incident electrons. Also of importance with regard to this factor are the melting and vaporisation temperatures of the material. Once melting occurs, the beam exerts pressure on the liquid interface, as do also evaporating molecules of the work material. Forces resulting from this latter effect are said to be due to *recoil* pressure. Quite apart from the complicated dynamical problem at the liquid interface, the beam and recoil pressures will have a marked effect on the rate of vaporisation of the work material. In the present state of the art, complications arising from the onset of melting are usually omitted from consideration in the design of electron beam machines although they are of the utmost importance in connexion with the machining mechanism, as will be discussed in a later section of the paper. Further, in design considerations, it is assumed that the thermal diffusivity and conductivity are constants independent of temperature. The various factors which influence the dimensions of the heat-affected zone will now be considered in a little more detail.

2.1. Current Distribution in the Focused Beam

The rms diameter of the focused electron beam on the work material is determined by the electron optical system and its aberrations. Fig. 1 shows the basic parts of the usual type of
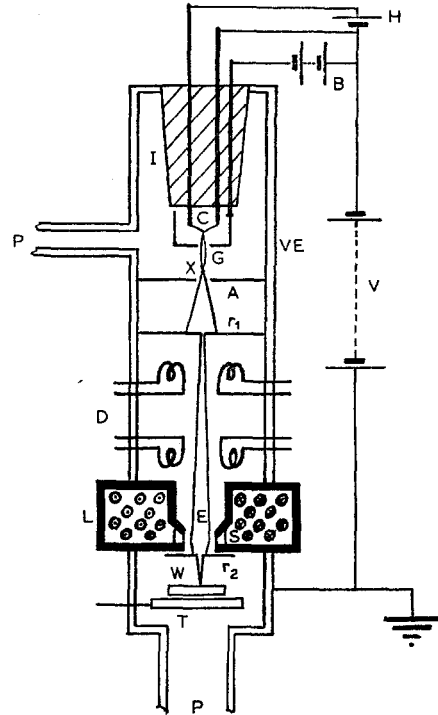

Figure 1 Basic configuration of an electron beam milling machine. (A) anode aperture; (B) grid bias supply or pulse generator; (C) tungsten hair-pin cathode; (D) double deflection coil system; (E) electron beam; (G) grid aperture; (H) cathode heater supply; (I) high voltage insulator; (L) magnetic focusing objective lens; (P) vacuum pump; (r_1, r_2) beam limiting apertures; (S) vacuum seal; (T) adjustable work-table; (V) high voltage supply; (VE) evacuated vessel; (X) electron gun crossover spot; (W) work-piece.

electron beam milling machine. In all present machines, the source of electrons is a tungsten hair-pin cathode. Although thoriated tungsten and oxide cathode give more emission at a given temperature, they are not suitable for use in these machines because of the high voltages used. They would be destroyed by positive ion poisoning. Electrons from the tip of the cathode are focused into a *cross-over* spot, smaller than the cathode tip itself, by an electron gun. The characteristics, and necessary conditions to obtain maximum current density in the crossover, have been investigated by Haine and Einstein [4], and by Brown [5]. A demagnified image of this cross-over spot is then formed by a magnetic objective lens on the work material. This image, in the absence of aberrations, is termed the *Gaussian* spot. The distribution of

beam current within this image is approximately *Gaussian** and can be described by an rms diameter d_0.

The diameter, d_0, is equal to the cross-over diameter, d_g, multiplied by the magnification, M (< 1), of the objective lens. Provided the beam current is not allowed to fall, it would appear that the current density in the final spot could be made indefinitely large by making d_0 sufficiently small, that is M sufficiently small by making the objective sufficiently powerful. However, this takes no account of aberrations in the system which will now be considered.

2.1.1. A Fundamental Limitation on the Maximum Current Density

Electrons are emitted from the cathode tip with a Maxwellian spread in energy corresponding roughly to the temperature of the cathode. Langmuir [6] has shown that this imposes a limitation on the maximum current density which can be obtained in any focused image of the cross-over spot. In the present case, where the semi-angle, α, which the beam subtends at the final image, is small, and where the energy, qV, of the incident electrons is large compared with kT, k being Boltzmann's constant and T the cathode temperature in ° K, the maximum current density in the focused image is

$$j = j_c \left(\frac{qV}{kT}\right) \alpha^2 \qquad (1)$$

where j_c is the current density at the cathode tip. The maximum current in the image is therefore given by

$$I = j_c \left(\frac{qV}{kT}\right) \alpha^2 \times \frac{\pi}{4} d_0^2 \qquad (2)$$

The maximum cathode current density, j_c, is limited to about 2 A/cm² by the maximum temperature of about 2800° K at which the cathode can be operated. At higher temperatures the *life* of the cathode would be prohibitively short. The maximum semi-angle, α, is limited, in a way which will be discussed shortly, by the spherical aberration of the objective. It is thus only possible to increase the current density in the image by increasing the accelerating voltage, V. The maximum value of V is limited by the expense and difficulty of working with very high voltages and by electron penetra-

tion effects, which will also be discussed later. In practice, the highest voltages used have been about 150 kV, while for thin film machining the limit is about 60 kV.

2.1.2. Spherical Aberration in the Objective

Each point in the cross-over spot is focused not to a point in the image but rather to a disc of least confusion of approximately *Gaussian* form given by [7].

$$d_s = \left(\tfrac{1}{2}\right) C_s \alpha^3 \qquad (3)$$

where C_s is a constant of the objective lens at a given focal length, f. Liebmann and Grad [8] have shown that C_s may be written as Cf, for magnetic iron shrouded coil lenses, where C is a constant dependent only on the form of the lens. For most electron beam machines, C_s would be in the range 1 to 10 cm.

The difficulty of increasing the current density by decreasing the magnification, M, is now apparent. As M decreases, α increases and so does the effective diameter, d, of the image. There is, however, an optimum α, or d_s, for which the current density is a maximum, as will now be discussed. It has been shown by Wells [3] that rms diameters should be added in quadrature, and thus the rms diameter, d, of the focused image, allowing for spherical aberration, is given by

$$d^2 = d_0^2 + d_s^2 \qquad (4)$$

From equations 2, 3 and 4, the maximum mean current density over the diameter, d, is

$$j = j_c \left(\frac{qV}{kT}\right) \frac{(d^2 - \tfrac{1}{4} C_s^2 \alpha^6)}{d^2} \alpha^2 \qquad (5)$$

Considered as a function of α, with d held constant, this has a maximum of [9, 10]

$$j_{max} = 0.75 j_c \left(\frac{qV}{kT}\right) \left(\frac{d}{C_s}\right)^{\tfrac{2}{3}} \qquad (6)$$

which occurs when d is equal to $2d_s$, that is when d_0 is equal to $\sqrt{3} \, d_s$. Alternatively, equation 5 may be expressed in terms of d_0 instead of d. The current density may then be optimised [11] with respect to α, holding d_0 fixed. The value of j_{max} is then slightly lower. The difference between these techniques has been discussed by Brown [5].

Gaussian is used in two different senses here. In the first instance, it refers to *Gaussian* optics, that is aberration-free optics, and in the second to a *Gaussian* statistical distribution.

2.1.3. Other Aberrations

Other aberrations in the system are not significant provided the accelerating voltage and the lens excitation current have adequate stability. This usually amounts to a stability of a few parts in 10^4, which requires careful design [12, 13] in the case of the high voltage supply. This is because of the possible occurrence of corona discharge. There are also aberrations associated with the deflection of the beam. So far, these have not received a lot of attention, the practice being to limit the deflection of the beam to angles at which such aberrations are not troublesome. It must be pointed out, however, that it is necessary for the beam to pass axially through the components of the electron gun and through the pole pieces of the magnetic lenses, otherwise parasitic aberrations are likely to arise. In the design of a machine, provision must be made for the accurate alignment of all lenses.

Experimental studies [4, 5] indicate that current densities in the final image within an order of the maximum predicted values are readily obtainable in practical machines.

2.2. The Transfer of Energy to the Work Material

Having discussed the conditions necessary to optimise the current density in an image of given diameter, the details of the energy transfer with, and of the temperature produced in, the work material must be considered.

2.2.1. The Disc Heating Model

The simplest assumption is to say that the energy of the beam is absorbed in the surface layer on which it is incident. This is called the *disc heating model*. In addition, it is assumed that, apart from the absorption of the beam energy, no other transfer of energy across the free surface of the work material occurs. An analytical solution of the steady state heat conduction problem for this model has been given by Vine and Einstein [14] for a semi-infinite solid. They found that, with a beam of *Gaussian* distribution, the peak temperature at the centre of the distribution was given by

$$\theta_0 = \frac{0.099 \, VI}{\sqrt{\pi} \, Kd} \qquad (7)$$

where I is the beam current and K is the thermal conductivity of the material. In addition, the

rms diameter of the temperature distribution, in the surface and perpendicular to it, was not significantly different from that of the focused beam. Using equation 6, the peak temperature rise can be expressed in terms of the voltage, V, and the beam diameter, d, for the condition of optimum current density in the focused beam. Thus,

$$\theta_0 = 0.033 \, j_c \left(\frac{q}{kT} \right) \frac{1}{KC_s^{\frac{2}{3}}} V^2 d^{\frac{2}{3}} \qquad (8)$$

an optimistic result, since electron penetration and backscatter have not been considered.

A mixed analytical and numerical method solution for the transient conduction problem using the disc heating model has been given by Pittaway [15]. This author gives results for both the semi-infinite solid and for a semi-infinite thin film. He considers the rise of temperature following the incidence of a pulsed beam and the subsequent fall of temperature after removal of the pulse. In addition, he considers the case of a continuous beam moving through a point on the target. A similar analysis has been given by Taniguchi and Maezawa [16]. Again, these analyses predict too high temperatures because of the neglect of electron penetration and backscattering effects.

2.2.2. The Source Dispersal Effect and the Power Retention Factor

The penetration of the beam and the scattering of the electrons within the target is known as the *source dispersal effect*. In addition, some of the electrons may ultimately be scattered back out of the surface of the target and their residual energy lost to the heating process. The fraction of the incident energy retained by the work material is termed the *power retention factor*, p. Vine and Einstein [14] have used the Archard [17] model of electron penetration and scattering, in conjunction with the Thomas-Whiddington law for the energy loss of the electrons in the material, to examine the source dispersal effect and power retention factor. They solved a finite difference version of the steady state heat conduction equation, that is Poisson's equation, over a two-dimensional mesh. The results are presented in the form of a correction to the steady state solution of the disc heating model. thus the peak temperature, θ_0, is expressed as

$$\theta_0^1 = P \, \bar{U}_0^* \, \theta_0 \qquad (9)$$

where p is the power retention factor and

$\bar{U}_0^*$ is the fractional correction to θ_0 of equation 8, to allow for the source dispersal effect. Their results are most conveniently represented by figs. 2 and 3 which are reproduced from their paper (figs. 4 and 6). The power retention factor, p, is independent of the accelerating voltage and $\bar{U}_0^*$ is independent of target material provided it is expressed as a function of the ratio of electron range in the material to focused beam spot diameter. Figs. 2 and 3 are therefore universal curves applicable in any circumstances.
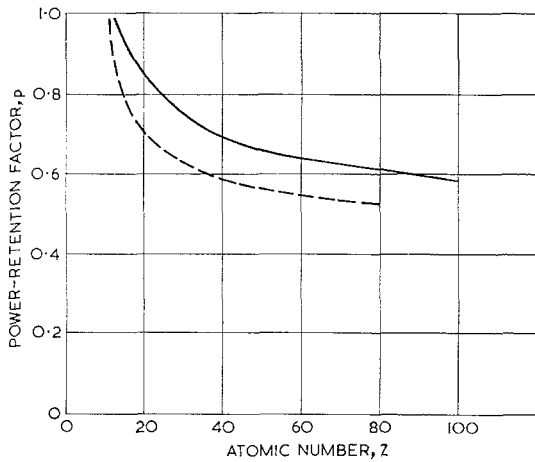
Figure 2 Fraction, p, of incident power absorbed by the target as function of atomic number, Z.
———————— Power-retention factor, p
———————— Electron (number) retention factor $(1-N)$ (Archard)
(By courtesy of J. Vine and P. A. Einstein.) (Reproduced from Proc. IEE, Vol. III, No. 5, May 1964, p. 925.)
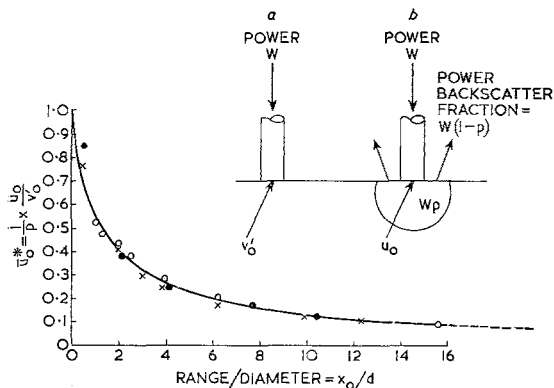

Figure 3 Universal curve for temperature rise in any material as function of electron range in diameters. (a) disc heating model; (b) with source dispersal effect.
(By courtesy of J. Vine and P. A. Einstein.) (Reproduced from Proc. IEE, Vol. III, No. 5, May 1964, p. 925.)

One of the more important conclusions to be drawn from this work is that increases in beam power made to achieve higher temperatures are best accomplished by increasing the beam current, rather than the beam voltage, in order that $\bar{U}_0^*$ may be kept as close to unity as possible. As a concluding remark with regard to Vine and Einstein's work, it is to be noted that they use linear rather than quadrature addition of the diameters, d_0 and d_s, see equation 17 of their paper and Brown [5], and therefore their results underestimate the maximum temperature by a factor of approximately two. This throws some doubt on their apparent excellent correlation between theory and experiment. However, the Archard model itself is only a crude approximation to electron penetration and scattering effects, and close correlation between theory and experiment would appear to be fortuitous. Another consequence of the source dispersal effect is that the rms diameters of the temperature distribution become appreciably greater than the beam diameter, and different in the radial and normal directions. Thus, for a 2 μm diameter beam, curves given by Vine and Einstein indicate a radial rms diameter of about 8 μm and a normal rms diameter of about 10 μm.

The transient heat conduction problem, allowing for the source dispersal effect and power retention factor, for a pulsed electron beam has been considered by Wells [3]. This author presents a simplified but approximate method of analysis based on the quadrature addition of the rms diameters of the various effects. Thus, in the radial direction, he adds in quadrature diameters due to thermal conduction, source dispersal effect, spherical aberration and Gaussian spot size, while in the normal direction diameters for thermal conduction and source dispersal effect only are considered. The thermal conduction rms diameter is taken as 2.35 $\sqrt{mt}$ where m is the thermal diffusivity of the material and t is the time. This is derived from the analytical solution for the point source-semi-infinite solid transient problem. An attempt is made to use an improved model for the source dispersal effect based on experimental observations and data but subsequent approximations probably led to results no more exact than those predicted on the Archard model. In any event the power retention factor as determined by Vine and Einstein is used. By maximising the energy transferred to the material from the beam

101

in a time, t, for a given radial rms diameter of temperature distribution, optimum values of the design parameters are deduced. These are

$$V = 9.17 \times 10^5 (\rho\, d)^{0.606} \text{ volts}$$
$$d_0 = 0.582\, d$$
$$\alpha = 0.877\, C_s^{-\frac{1}{4}}\, d^{\frac{1}{4}} \tag{10}$$
$$t = (0.0615/m)\, d^2$$

where ρ is the density of the work material. The beam current is then

$$I = 2.18 \times 10^9 \left(\frac{j_c}{T}\right) p^{0.606}\, C_s^{-\frac{1}{4}}\, d^{3.27} \text{ amps} \tag{11}$$

and the peak temperature attained is

$$\theta_{\max}^1 = 6.64 \times 10^{13} \frac{p\rho^{1.212}\, j_c}{TKC_s^{\frac{3}{4}}}\, d^{2.88} \tag{12}$$

This is, however, an approximate design technique and can be expected to predict the parameters for optimum operation under pulse conditions only to within an order of magnitude.

It is to be noted that, as yet, very little theoretical work has been carried out on thin conducting films deposited on low conductivity substrates with due allowance for source dispersal and back scatter. Transient analyses, in these cases, are particularly needed, since pulsed beam operation would appear to be even more advantageous than for semi-infinite solids.

2.2.3. Numerical Examples

To conclude this section, a few numerical calculations will be made to indicate the magnitude of temperatures to be expected in practical circumstances. Initially, steady state conditions will be considered and the machine will be assumed to have a minimum spot size of 3 μm, a spherical aberration constant, C_s, of 2 cm, and an accelerating voltage of 50 kV. In addition, it will be assumed that the operation of the machine has been optimised to produce the maximum possible temperature rises. On the disc heating model, equation 8 then predicts a θ_0 for aluminium of approximately 1100° C, and for tungsten of approximately 1500° C. At any accelerating potentials, fig. 2 gives the power retention factors for aluminium and tungsten as approximately unity and 0.63 respectively. For a voltage of 50 kV the electron ranges in aluminium and tungsten are about 24 μm and 4.2 μm respectively. Fig. 3 then gives the fractional correction $\bar{U}_0^*$ to θ_0 for the two cases as 0.18 and 0.53 respectively. The peak temperature for the 3 μm spot is thus about 200° C for aluminium and about 500° C for tungsten.

According to equation 8 the temperature, θ_0, is proportional to the square of the voltage, V. However, the electron range as given by the Thomson-Whiddington law is also proportional to the square of the voltage, V. Reference to fig. 3 thus shows that the correction factor, $\bar{U}_0^*$, decreases with increasing voltage and hence θ_0^1 (equation 9) increases less rapidly than θ_0 with the accelerating voltage. For example, if the voltage is doubled to 100 kV, θ_0^1 approximately doubles to 400° C for aluminium, and increases by a factor of about 2.5 to 1250° C for tungsten.

Again, according to equation 8, the temperature, θ_0, increases as the five-thirds power of the spot diameter, d, but θ_0^1 increases even more rapidly because, as reference to fig. 3 shows, the correction factor $\bar{U}_0^*$ increases as the diameter, d, is increased. For example, the temperature of 200° C which was estimated previously for aluminium is increased by a factor of 4.75 when the spot size is increased from 3 μm to 6 μm.

Considering now the case of pulsed beam operation of a machine with a spherical aberration constant of 2 cm, equation 12 predicts a peak temperature, $\theta_{\max}^1$, of 200° C and 500° C for aluminium and tungsten when the spot diameters are approximately 7 μm and 4 μm respectively. The optimum voltages and pulse durations for these spot diameters are given by equation 10 as about 20 kV and 2×10^{-8} sec for aluminium and 50 kV and 3.5×10^{-8} sec for tungsten. These figures correspond to the optimum energy transfer condition, and it would not always be convenient to operate a machine under this condition. For example, higher temperatures, and incidentally larger spot sizes, would result if the pulse durations were increased.

3. The Design of Electron Beam Milling Machines

To produce the high energy electron beam of small cross-sectional diameters necessary to facilitate machining of materials, three basic requirements exist in the construction of the electron beam machine. These are: firstly, a vacuum system providing sufficiently low pressures to allow the emitted electrons a long mean free path; secondly, an electron gun to produce the high powered electron beam; and, finally, a focusing system to reduce the beam diameter, in order to provide the necessary power densities for machining. All electron beam milling machines reported to date include certain refinements

associated with the particular task which the machine was intended to perform, but the basic requirements stated earlier remain the same.

Ultra-high vacuums are not essential either for the production of electron beams or for the milling process. Most machines use pressures of between 10^{-4} and 10^{-6} torr and these are achieved by conventional methods. Such methods are well explained in books by Dushman [18] and Pirani and Yarwood [19].

Many electron gun configurations are possible for the production of the electron beam. The voltage on the anode of the electron gun provides the accelerating voltage to the electron beam. Since alignment is very important in these machines, triode systems are generally preferred to multi-electrode systems. Three systems have been considered applicable: the simple triode with plane or cylindrical grids and anodes; the Pierce-type [20] system with concentrically spherical electrodes; and the Steiger-wald [2] gun which has a conically-shaped grid closely surrounding a hair-pin-shaped filament. Line diagrams of these are given in fig. 4. Both the Pierce and Steigerwald systems form cross-over spots, which form the objects for the focusing system, appreciably beyond the anode, so necessitating a long machine column. Such guns are also critically dependent upon perfect alignment, and for this reason most electron beam machines use the simple triode system.
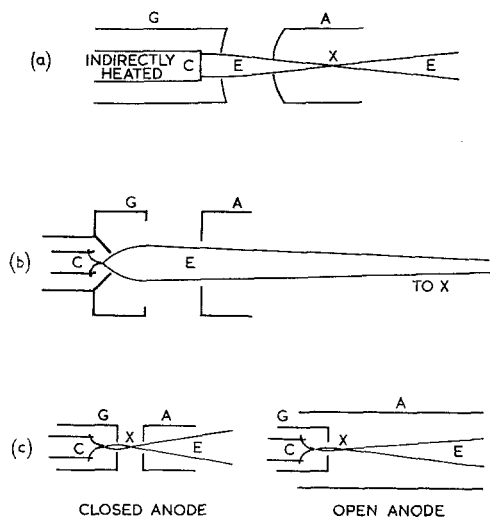

Figure 4 Line diagrams of suitable electron guns: (a) Pierce gun configuration; (b) Steigerwald gun configuration; (c) normal triode systems. (A) anode; (C) cathode; (G) grid; (E) electron beam; (X) cross-over spot.

As mentioned previously, tungsten hair-pin cathodes are generally used as the electron source. The emission is critically dependent upon the filament temperature, which is readily controllable, this being a great advantage in experimental machines. Some investigation has been performed into the use of field emission cathodes as electron sources, but at the time of writing, all reported electron beam machines use tungsten hair-pin filaments.

Accelerating voltages have usually been decided according to the purpose of the machine itself. A brief discussion of this has been given in the preceding section. Obviously, lower-powered machines are cheaper and easier to construct, but, as yet, no conclusive evidence is available as to the relative merits of high and low voltage machines.

Electron beam machines are normally pulsed by means of the grid of the electron gun, the grid voltage being taken from beyond the cut-off value to a value corresponding to optimum beam current. For hair-pin cathode guns this optimum occurs when the grid is still somewhat negative relative to the cathode [4, 5]. Hence the electronic circuitry associated with the electron gun is quite considerable. The experimental work of Haine and Einstein [4] and of Brown [5] indicates that adequate beam current can be obtained from a plane disc triode electron gun, with hair-pin cathode, for electron beam machining purposes, and, further, that this current can be suitably controlled.

In the design of a focusing system, two possibilities are present, the use of electrostatic or electromagnetic lenses. Electrostatic systems require high voltages and the field in the region of the work-piece may become non-uniform during the machining process. Such systems are only used for the very low power machines used in electron-beam-assisted chemical etching. Electromagnetic systems are used in all reported thermal milling machines.

Each magnetic lens consists of a coil of wire surrounded by an iron or steel shroud, an intense field being present in the region of a narrow gap and pole piece in the shroud. Liebmann and Grad [8] have evolved a formula relating the focal length, f, of a lens to its geometrical design, the excitation current, I, and the accelerating voltage, V, given by

$$f = \frac{50 \, (D \, S)^{\frac{1}{2}} \, V}{(NI)^2} \qquad (13)$$

103

where D is the lens bore diameter, see fig. 5, S is the pole gap width, and N is the number of turns in the coil.

The spherical aberration constant, C_s, also depends upon f, D and S [7]. However, the spherical aberration spot diameter, d_s, is proportional to the cube of the beam half-angle, α, see equation 3, and so it may be reduced by stopping the beam down despite a large value of C_s. Unfortunately, reducing α also reduces the current density and hence the lens poles must be critically designed for the lowest C_s while maintaining the required focal length. In addition, iron saturation must be prevented by ensuring that the iron shroud is sufficiently thick. A cross-section of a typical lens is shown in fig. 5.
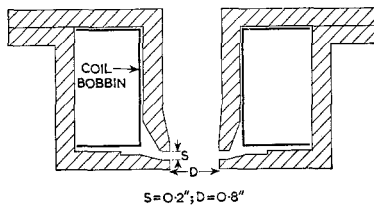

$$S = 0.2''; D = 0.8''$$

Figure 5 Cross-section of typical electromagnetic lens shroud.

Normally a single magnetic lens provides sufficient demagnification for electron beam milling, but often a two-lens system is employed since this provides a facility for altering the Gaussian spot size without altering its power density.

To use the electron beam energy to its best advantage, the point of incidence of the beam on the work-piece must be moved so as to follow the required profile of cut. This may be achieved in two ways, by mechanical movement of the work-piece, or by electromagnetic deflection of the electron beam itself.

Movement of the work-table by mechanical means gives less precision than beam deflection, but it is useful because the area of scan of the electron beam without defocusing is very small, and movement of the work-piece together with beam deflection can facilitate the machining of quite large areas. The beam can be deflected by about 1 mm in most cases without significant defocusing. In order to ensure that the beam passes axially through the poles of the final lens, it is either deflected after passing through

the final lens or a double deflection system is used before the final lens. This consists of two sets of quadrupole lenses at different points along the axis of the machine. The first set deflects the beam in one sense and the second set in the opposite sense, such that it crosses the axis at the plane of the final focusing lens. Systems have been proposed [13, 21] for programmed automatic control of beam deflection and table movement, such that the machining of any given profile can be carried out. Up to the present time, however, no reports on the operation of such systems have appeared. Most reported machines include an accurate work-table moving arrangement and some machines have a limited number of simple programmes for the deflection of the beam and movement of the table.

Some facility is necessary on an electron beam machine to view the work-piece during, and immediately after, the machining process. This is generally achieved by optical means, but proposals [22] have been made to use the beam, at lower power and with smaller spot size, as the beam of a scanning electron microscope at convenient intervals between periods of machining.

Some typical electron beam milling machines will now be briefly described.

3.1. Carl Zeiss [23]
The Carl Zeiss Co, of Oberkochen, Germany, were the first to do extensive research into electron beam milling machines and produced the first commercial model in the late 1950s. The machine, see fig. 6, uses a Steigerwald [2] electron gun and a single lens focusing system. It has accelerating voltages of up to 150 kV with a maximum power density of 10^9 W/cm². The beam can be pulsed at frequencies of up to 10 kc/s. The work-piece is viewed directly from above by means of a microscope suitably positioned on the column. Maximum beam currents of 0.8 mA are available for continuous beam operation, but for pulse duration a much higher current is possible. A beam deflection system capable of cutting simple shapes is provided.

3.2 El-Kareh [24]
El-Kareh of RCA has described a machine which, like the Zeiss machine, was designed as a versatile general purpose tool. This machine was developed from the RCA EMU 3A
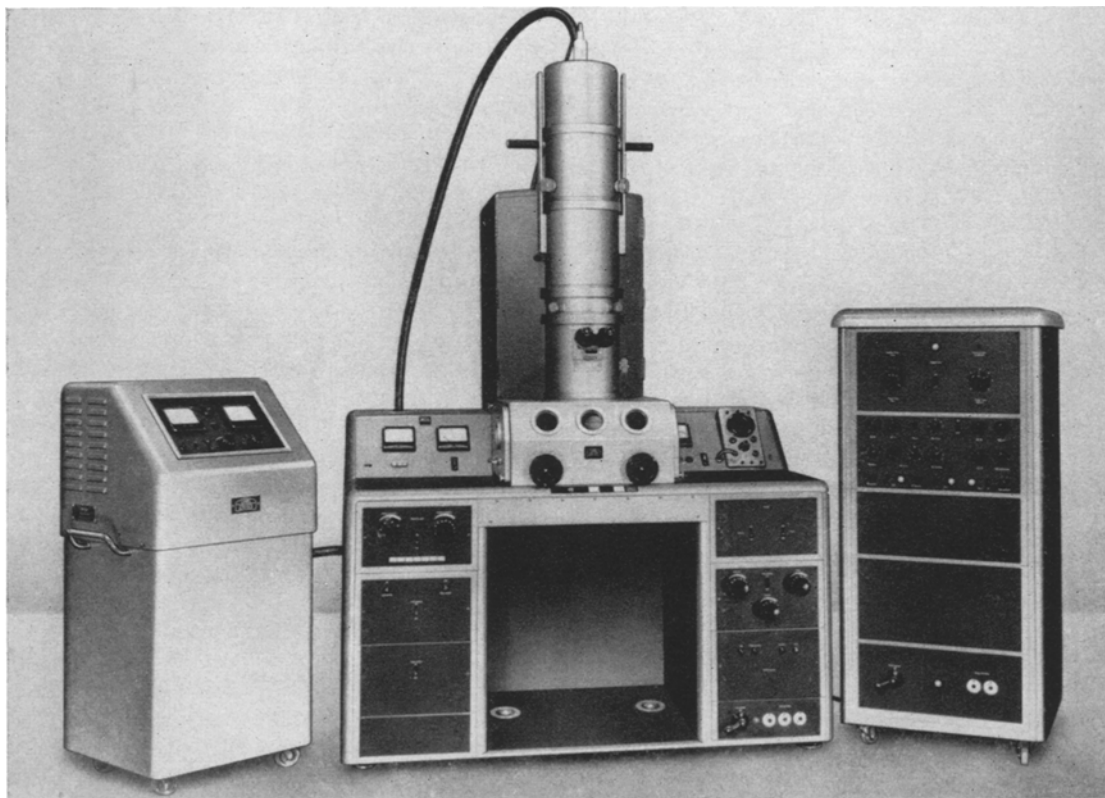
Figure 6 The Carl Zeiss electron beam milling machine. Electron beam machine, type BFM 100. Seen from left to right: high-voltage supply 150 kV, 100 W; electron beam machine with vacuum system; control cabinet for electron deflector control.

(By courtesy of the Carl Zeiss Co, Oberkochen, West Germany.)

electron microscope. A standard triode gun system is used together with a two-lens focusing system. The maximum anode voltage is 100 kV. Several viewing ports, a simple deflection system, and a versatile work-table are incorporated. A maximum current of 5 mA in a 25 μm spot diameter is shown to be theoretically possible, but this has not been achieved in practice.

3.3. Einstein [11]

Whilst at AEI, Einstein developed a non-commercial experimental electron beam milling machine. It was designed for a wide range of functions but most of the experimental work has been concerned with *micromachining*. The machine operates at voltages of 30 to 60 kV with a maximum beam current of 100 μA and minimum spot size 1.5 μm. It has a deflection system with a linear scan of maximum velocity 40 cm/sec. An optical system enables the work-

piece to be viewed from above down the axis of the machine. Useful facilities for the rapid changing of the apertures and for moving the specimen are incorporated.

3.4. Perkins [25]

Perkins of The Plessey Co has designed and constructed a milling machine specifically for the application of micromachining with special reference to microelectronic circuits. This machine uses an accelerating voltage of 20 kV, and draws a total current of 3 mA. Experiments on milling, welding and alloying have been performed successfully. Scanning of the beam using simple waveforms have been achieved together with mechanical movement of the work-piece. Viewing is achieved down the column of the machine with the aid of a *just-off-axis* mirror. Results show that low voltage machines are useful in microelectronic circuit construction techniques.

105

3.5. Kelly and King [22]

Kelly and King of the Mullard organisation have developed a high power general purpose machine. The usefulness of electron beam milling for many applications in the electronics industry is being investigated with this machine. The machine basically consists of a triode gun capable of giving 20 mA total current, at voltages from 15 to 150 kV. A single lens system and a double deflection system are used. Viewing is achieved by an optical system level with the specimen with the aid of an oblique mirror placed very close to the specimen. A secondary emission scanning microscope facility has recently been added, which uses the same beam, at a lower intensity. Spot sizes down to 3 μm have been obtained.

3.6. Millard [26]

Millard has described a machine in use at RRE, Malvern. This machine was designed essentially as a low-voltage machine for microelectronic circuit processing. It was developed from an X-ray projection microscope and was constructed by Electron-Physical Instruments Ltd. It uses a 20 kV accelerating voltage and 20 to 100 μA beam current in a 10 μm minimum spot diameter. The electron gun is at the base of the column and the specimen is at the top. Viewing is achieved from above, i.e., from the opposite side of the specimen to the incident beam. Such a system is only suitable for viewing machining processes on thin films for which the machine has mostly been used.

3.7. Southampton University

The Southampton University machine, designed by the authors, is being applied to microelectronic circuit construction and in particular the machining of thin films. A normal triode electron gun is used with a maximum voltage of 30 kV and current of 2 mA. A two-lens focusing system is employed. The machine was designed such that any part could quickly be modified or replaced. Viewing is achieved through the thin film by a simple optical system. Optimum beam conditions were found and a minimum spot size of 7.5 μm has been achieved with a beam current of some 100 μA.

4. Results of Experimental Work with Electron Beam Machines

Electron beam thermal milling is capable of a working precision of the order of 1 μm. It has been used as an alternative to conventional milling and grinding techniques which, in their more refined forms, have a similar precision. In particular thermal milling has been used for the machining of titanium aircraft engine parts. In one application, the electron beam was used to weld a plug of titanium into an incorrectly positioned borehole in a large titanium casting. The same beam was then used to mill the plugged region and to bore the required hole in the correct position. Titanium is an expensive, high-melting-point metal and the cost of moderately-sized, machined castings may run into several thousands of pounds. The saving which may be effected by the electron beam machine in this error-correcting role could be appreciable.* Another milling process having approximately the same working precision is *spark erosion* [27]. This latter process has the advantage, compared with electron beam machining, of not requiring the work-piece to be in a vacuum. However, it has the disadvantages of requiring a dielectric liquid between the work-piece and the spark electrode and of the erosion of the spark electrode itself, which is particularly troublesome when machining at the highest precision. At the present time, it would seem that spark erosion is a stronger competitor than electron beam milling for ultra-fine machining in what might be termed conventional milling applications. The particular advantage of electron beam milling, which might change this situation, is the complete lack of erosion of working tool, namely the electron beam. In both spark erosion and conventional milling, the working tool is gradually eroded away. A final advantage of electron beam milling is that there is every hope that the precision will improve with subsequent improvements of electron optical design. It is difficult to visualise comparable improvements in spark erosion and conventional techniques.

Currently, the principal applications of electron beam thermal milling are the cutting of apertures of some required form in self-sup-

*This work was reported at a Symposium in London, in 1961, which was organised by Degenhardt and Co Ltd to introduce the Carl Zeiss electron beam machines into this country. Unfortunately, there were no written accounts of the proceedings of this Symposium. Apparently, the work was carried out under the auspices of the Hamilton Standard Corporations in the USA. An extensive search of the literature has failed to produce a written record of this work, or of any other similar applications. There are many reports on the use of electron beams in industrial welding applications, but these are outside the scope of the present review.

porting thin foils or wafers, and the *selective etching* of deposited thin films on glass or ceramic substrates. One application of importance of the former category is the production of *out-of-contact* masks for vacuum deposition work. These masks are required to define accurately the edges of deposited films with particular applications such as the construction of some forms of microelectronic circuits and the construction of magnetic and cryogenic memory planes for computers. In the case of *selective etching* of thin films on substrates, the requirement is to accurately shape and to define the edge of the film without undue damage to the substrate itself. Again, the main application is to microelectronic circuit production. In both cases, the technique is in competition with the well-known [28] photo-mechanical* process which is capable of producing an edge definition of the order of 1 μm. It would appear that there is little hope that this latter definition can be improved, but as previously mentioned, there is every hope of improving the precision of electron beam milling.

4.1. The Machining of Self-supporting Thin Foils

A considerable amount of experience has been gained in the machining of thin self-supporting foils. Thus Opitz [23] and Steigerwald [29] have cut 1 mm slots in 75 μm thick foils in a number of high melting point materials using the powerful Zeiss machine. The edge definition of these slots is of the order of a few μm. They are, therefore, able to produce out-of-contact masks suitable for some of the not-too-miniaturised microelectronic circuit work. Perkins [25] has cut similar slots in 50 μm molybdenum sheets with widths down to 100 μm and with an edge definition of better than 10 μm. The slots cut in foils of this thickness are usually tapered, being narrower on the bottom side of the foil than on the top, but this is not necessarily a disadvantage for foils which are to be used as vacuum deposition masks. Kelly and King [22], in addition to cutting slots in metal foils, have cut masks in 6 μm thick silica sheet. They have discussed results for slots of widths of 1.5 and 20 μm and so confirm the competitiveness of the technique in comparison with the photomechanical process. A typical example of such

a mask is shown in fig. 7. Mather-Lees [30] has reported 10 to 12 μm wide slots cut in 6 μm thick nickel foils. Detailed examination of these foils often shows appreciable heat-affected zones, piling up of molten metal and recrystallisation effects, on either side of the slots. These zones may extend for distances of some 5 μm or so from the edges of the slots.

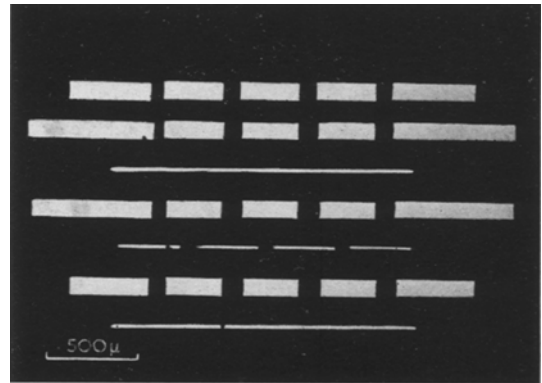Figure 7 Electron beam etched mask in 150 μm thick silica.
(By courtesy of J. Kelly and H. N. G. King, and Pergamon Press Ltd.)

4.2. The Selective Etching of Thin Films

Again, this topic has received appreciable attention. Opitz [23] and Steigerwald [29] were first to report work on the selective etching of thin films, but they give little detail on the thickness of the films concerned and of the substrates used. Among the films of substances they investigated were gold, lead sulphide, and nichrome. In the use of the latter, they have produced *meander* track resistors, see fig. 8. Einstein [11] has produced tantalum meander track resistors with slot widths down to 5 μm. One feature of the tracks cut in tantalum is a herringbone pattern, pointing along the direction of the beam motion, at the edges of the cut indicating a disruption of the film. Appreciably affected zones on either side of the track are often produced. Reduction of the beam power and a correspondingly lower scanning rate produces a cut of approximately the same width, but often with less area of affected zone on either side of the cut.

---

*Photo-chemical is probably a better term for this process. However photo-mechanical is the term by which the process is generally known.
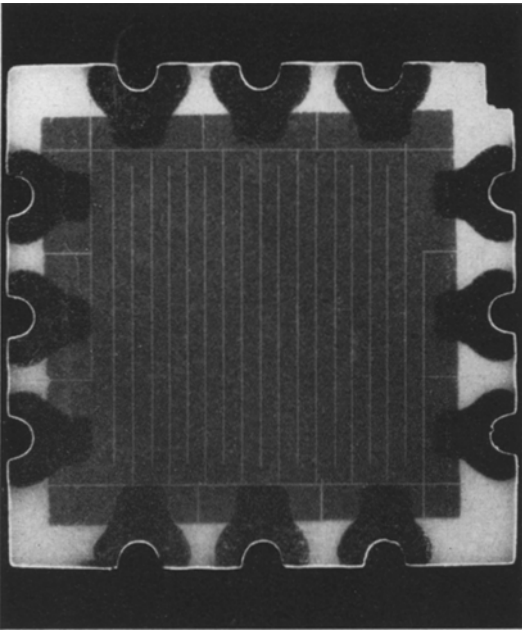
Figure 8 Electron beam etched meander track resistor. Resistor wafer with electron-beam surface millings. Width of lines 0.0004 in, magnification ×8.
(By courtesy of the Carl Zeiss Co, Oberkochen, West Germany.)

Local damage to the glass substrates and affected zones at the edges of the cuts have also been observed and discussed by Mather-Lees [30] and by Kelly and King [22]. Perkins [25], working with nichrome films, has investigated the profile of tracks cut in the films with a Talysurf. He observed a *pile-up* of material on either side of the track, which was still present to some extent even when the beam power was so low as not to cut the film right through. He has also made some comparison of results using, firstly, a continuous beam; secondly, a pulsed beam. Under certain conditions similar results are obtained. The profiles of slots in thin films have also been studied by Millard [26], who observed that the pile-up of material at the side of the slot is more pronounced with soda glass substrates than with borosilicate ones. In the latter case, not only were better edges obtained to the slots, but local damage to the substrate was much reduced. He reports cuts of 15 to 20 μm width in 1000 to 6000 A U films of various materials. The best results were obtained for nichrome and magnesium. Gold, copper and aluminium proved the most difficult materials to

108

work. The Southampton University machine has been used to cut slots in films of gold, silver and aluminium, of about 1 μm thick, on borosilicate substrates. Some results of this work are shown in fig. 9. By altering the machining conditions, the width of the slot could be controlled between 10 and 60 μm. These slots were cut with continuous beam operation, the work table being scanned beneath the beam. The repeatability of the results was good and data were obtained which enabled a slot of any given width to be cut in a prescribed material. The pile-up of material at the edges of the slots was examined with the aid of a Talysurf and typical results are shown in fig. 10. Removal of the metal film and the subsequent Talysurf examination of the machined track on the substrate resulted in the profiles shown in fig. 11. The correspondence of the ridges at the edges of the cuts indicate that some *frothing* or *boiling* of the substrate occurs in the machining process. This latter effect is considerably less in the case of borosilicate glass substrates when compared with those of soda glass.
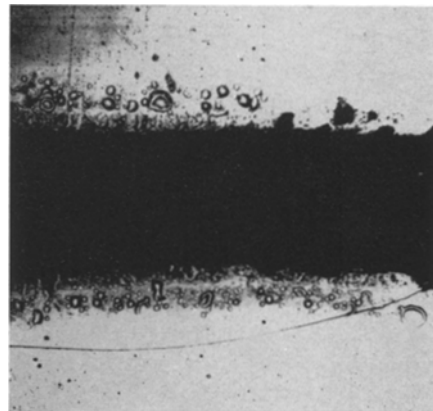

Figure 9 A typical electron beam etched slot. 2 μm thick aluminium film on borosilicate glass substrate; slot width 50 μm; spot size 20 μm; power density 3 × 10^5 W/cm^2; sweep speed 2.92 cm/sec (V_a = 25 kV, I_b = 40 μA) (magnification ×300).

5. Discussion of Results and the Mechanism of Machining

The discussion of the source dispersal effect and the results reviewed in this paper indicate that there is no advantage in using very high voltage beams for the micromachining of foils and thin films. Satisfactory experimental results have been achieved at voltages of 30 kV or less. The mach-
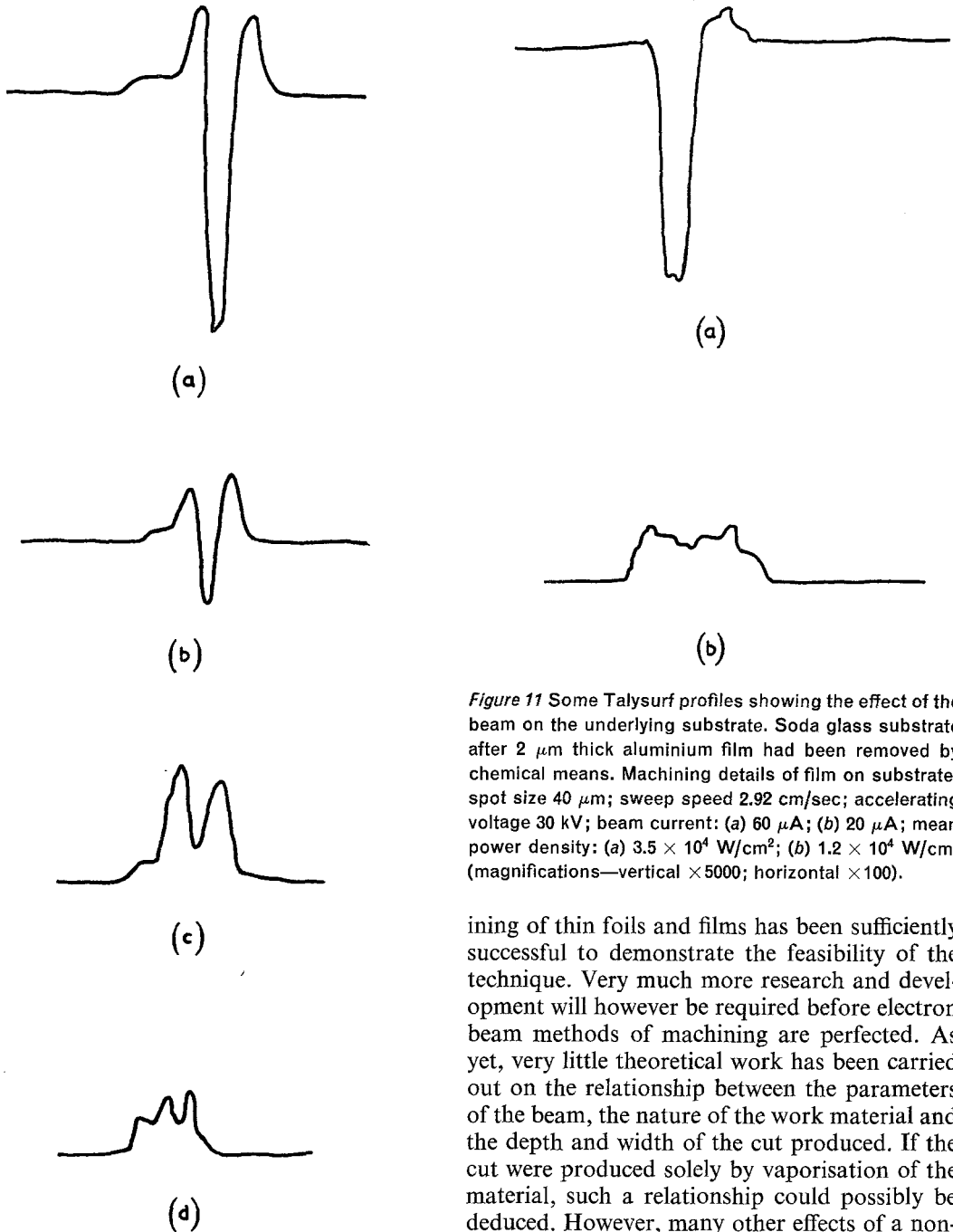
(a)

(b)

(c)

(d)

Figure 10 Some typical Talysurf profiles of the surface of an electron beam etched thin film. 2 μm thick aluminium film on soda glass substrate; spot size 30 μm; sweep speed 2.92 cm/sec; accelerating voltage 25 kV; beam current: (a) 60 μA; (b) 40 μA; (c) 25 μA; (d) 15 μA; mean power density: (a) 5 × 10^4 W/cm^2; (b) 3.3 × 10^4 W/cm^2; (c) 2 × 10^4 W/cm^2; (d) 1.2 × 10^4 (magnifications—vertical ×5000; horizontal ×100).

(a)

(b)

Figure 11 Some Talysurf profiles showing the effect of the beam on the underlying substrate. Soda glass substrate after 2 μm thick aluminium film had been removed by chemical means. Machining details of film on substrate: spot size 40 μm; sweep speed 2.92 cm/sec; accelerating voltage 30 kV; beam current: (a) 60 μA; (b) 20 μA; mean power density: (a) 3.5 × 10^4 W/cm^2; (b) 1.2 × 10^4 W/cm^2 (magnifications—vertical ×5000; horizontal ×100).

ining of thin foils and films has been sufficiently successful to demonstrate the feasibility of the technique. Very much more research and development will however be required before electron beam methods of machining are perfected. As yet, very little theoretical work has been carried out on the relationship between the parameters of the beam, the nature of the work material and the depth and width of the cut produced. If the cut were produced solely by vaporisation of the material, such a relationship could possibly be deduced. However, many other effects of a non-thermal nature are likely to occur.

Probably, vaporisation effects are of prime importance only when very high beam energies are used. The heat energy generated within the material raises its temperature and causes some evaporation. Some of this heat energy is also lost by conduction, radiation and convection [29]. Simple calculations show that only the

109

evaporation and conduction heat losses could be of any significance. Little conclusive evidence for massive evaporation of material exists, but conduction effects are of major importance. In all thin foil and film machining, the edges of the cuts are bordered by heat-affected regions which are probably due to conduction and the source dispersal effect. Possibly, materials of low thermal conductivity can be most successfully machined, as for these the conduction-heat-affected zone should be small. The work of Kelly and King [22] on silica tends to confirm this. However, the need does exist to be able to machine metals despite their high conductivities. For metals, therefore, it would seem advantageous to pulse the beam or to use fast scan rates in order to minimise the heat conduction loss.

As discussed in an earlier section in connexion with the source dispersal effect, electrons penetrate the work material and give up some of their energy well below the surface. For the case of the selective etching of thin films, this means that an appreciable part of the beam energy is dissipated not in the film but in the substrate. Vaporisation of the substrate material could possibly occur with consequent *blast-out* of material in molten or solid state. This effect has been recognised as occurring in high voltage electron beam welding, but has not been reported in connexion with lower voltage machines. Again, as considered in a previous section, the backscattering of electrons can cause heat to be liberated at, or near to, the surface of the metal outside the region actually covered by the beam, which is another possible reason for the affected area surrounding an etch.

The fact, that the substrate gets hot, causes thermal stress which could result in cracking of the substrate or could produce a ragged tear in the thin film. Most glass substrates, especially soda glass, have a high water content which outgasses when hot, explaining the *frothing* observed by Millard [26], and Brown [5]. The true value of electron beam etching of thin films will not be realised until stronger and more-heat-resistant substrates are used. Ideally, the best machining will be achieved on a material of high atomic number, low specific heat and low thermal conductivity, deposited on a substrate of low atomic number, high specific heat and high thermal conductivity. However, such an arrangement is difficult to achieve in practice.

At this point, it is convenient to mention another selective etching process which promises

advantages over the electron beam thermal milling method. It is the use of the focused beam of a high-powered, pulsed gas laser as a localised heat source. The advantage lies in that most of the beam energy will be absorbed in the metal film and very little will be absorbed in the transparent glass substrate. A disadvantage is that the machining precision is limited, theoretically, to the order of 1 μm. Work on this technique is being carried out in a number of laboratories and Forbes [31] shows photographs of 4 μm and 7 μm slots in thin films of nichrome and gold, respectively. As yet, no investigations of the profiles of the slots have been reported.

To conclude this section it might just be pointed out that electron-beam-assisted chemical methods are capable of selectively etching slots of a few hundred A U width in thin films but, as stated in the introduction, these methods are outside the scope of the present review.

Returning to a discussion of the results of figs. 10 and 11, it must be realised that, although the mass of an electron is minute, there are so many of them striking a target per unit time that they cause a significant pressure at the surface. This pressure is proportional to the change in momentum of the electrons and, since all eventually come to rest, the beam pressure is given by:

$$p = \frac{n\, m_e v}{t\, A} \qquad (14)$$

where (n/t) is the rate of arrival of electrons, m_e is the electron mass, v, the electron velocity, and A is the focused spot area, i.e. $(\pi d^2/4)$. Equation 14 is readily expressed in terms of the power density, W, in the spot as

$$p = W \bigg/ \sqrt{\left(\frac{2m_e}{qV}\right)} \qquad (15)$$

This pressure may be as high as a few atmospheres in high-powered electron beams. It is sufficient to cause a migration of molten material which recrystallises at the sides of the etch, which is a possible reason for the slot profiles. The effect of electron pressure has been discussed by Crawford [32].

Recoil pressure effects, due to escaping molecules, could also be significant if sufficient heat is present for evaporation from the surface of the material. This has been discussed by Crawford [32] and Wells [33].

Another possible machining method is described by Mather-Lees [30]. It depends upon the

mobility of surface molecules being increased by a momentum transfer process at the expense of the electron beam energy. He suggests that, above a certain rate, the energy of the electron beam may be absorbed quickly enough to cause a thermal runaway which quickly reaches evaporation temperature. Such an evaporation could possibly take place without affecting underlying layers.

Further work is necessary to determine which of these processes occur, and the conditions under which they are present, before any calculations of the profile and depth of the cut can be undertaken.

Acknowledgements

References

1. K. H. STEIGERWALD, *Proc. Fourth Congress on Electron Microscopy*, Berlin 1958 (1960) 276 (in German).
2. K. H. STEIGERWALD, *Optik* **5** (1949) 469 (in German).
3. O. C. WELLS, *IEEE Transactions on Electron Devices* **4** (1965) 224.
4. M. E. HAINE and P. A. EINSTEIN, *Brit. J. Appl. Phys.* **3** (1962) 40.
5. G. BROWN, Ph.D. Thesis, Electronics Department, University of Southampton (1965).
6. D. B. LANGMUIR, *Proc. IRE* **25** (1937) 977.
7. M. E. HAINE, "The Electron Microscope" (Spon, 1961).
8. G. LIEBMANN and E. M. GRAD, *Proc. Phys. Soc. (Lond.)* **64** (1951) 956.
9. T. E. EVERHART, Berkeley University, California, *ASD Technical Documentary Report* (1962) 63.
10. H. SCHWARZ, *Rev. Sci. Inst. (USA)* **33** (1962) 688.
11. P. A. EINSTEIN, *Proc. Microminiaturization Conference*, West Ham (1963) 178.
12. A. C. WILKINSON, *Microelectronics and Reliability* **4** (1965) 80.
13. S. PANZER and F. SCHLEICH, *Microelectronics and Reliability* **4** (1965) 117.
14. J. VINE and P. A. EINSTEIN, *Proc. IEE* **3** (1964) 921.
15. L. G. PITTAWAY, *Brit. J. App. Phys.* **15** (1964) 967.
16. N. TANIGUCHI and S. MAEZAWA, Alloyd Electronics Corp, *Proc. 5th Electron Beam Symp.* (1963) 135.
17. G. D. ARCHARD, *J. App. Phys.* **32** (1961) 1505.
18. S. DUSHMAN, "Scientific Foundations of Vacuum Technique" (Wiley, 1962).
19. M. PIRANI and J. YARWOOD, "Principles of Vacuum Engineering" (Chapman and Hall, 1961).
20. J. R. PIERCE, *J. App. Phys.* **11** (1940) 548.
21. G. R. HOFFMAN, *Microelectronics and Reliability* **4** (1965) 59.
22. J. KELLY and H. N. G. KING, *Microelectronics and Reliability* **4** (1965) 85.
23. W. OPITZ, Alloyd Electronics Corp, *Proc. 2nd Electron Beam Symp.* (1960) 32.
24. A. B. KAREH, *RCA Review* **XXIV** (1963) 5.
25. K. D. PERKINS, *Microelectronics and Reliability* **4** (1963) 35.
26. P. A. MILLARD, *Microelectronics and Reliability* **4** (1963) 25.
27. G. V. SMITH, *J. Brit. IRE* **22** (1961) 409.
28. H. G. MANFIELD, *Electronic Engineering* **35** (1963) 520.
29. K. H. STEIGERWALD, Alloyd Electronics Corp, *Proc. 3rd Electron Beam Symp.* (1961) 268.
30. S. MATHER-LEES, *Microelectronics and Reliability* **4** (1963) 71.
31. N. FORBES, *Microelectronics and Reliability* **4** (1963) 105.
32. C. K. CRAWFORD, "Introduction to Electron Beam Technology", edited by R. Bakish (Wiley, 1962), p. 315.
33. O. C. WELLS, "Introduction to Electron Beam Technology", edited by R. Bakish (Wiley, 1962), p. 354.